Hindawi
Journal of Chemistry
Volume 2017, Article ID 4102796, 11 pages
https://doi.org/10.1155/2017/4102796

Research Article

Novel Thiazole Derivatives of Medicinal Potential: Synthesis and Modeling

Nour E. A. Abdel-Sattar, Abeer M. El-Naggar, and M. S. A. Abdel-Mottaleb

Department of Chemistry, Organic Labs, and Computational Chemistry Lab, Faculty of Science, Ain Shams University, Abbasiya, Cairo 11566, Egypt

Correspondence should be addressed to Nour E. A. Abdel-Sattar; nourel-dinahmed@sci.asu.edu.eg

Received 17 March 2017; Revised 18 May 2017; Accepted 4 June 2017; Published 24 July 2017

Academic Editor: Pedro M. Mancini

This paper reports on the synthesis of new thiazole derivatives that could be profitably exploited in medical treatment of tumors. Molecular electronic structures have been modeled within density function theory (DFT) framework. Reactivity indices obtained from the frontier orbital energies as well as electrostatic potential energy maps are discussed and correlated with the molecular structure. X-ray crystallographic data of one of the new compounds is measured and used to support and verify the theoretical results.

1. Introduction

The thiazole has an important component effect of the pharmacophores of a large number of medicinal significance molecules and the evaluation of their biological activity, such as antibacterial [1], antiprotozoal [2], antitubercular [3], antifungal [4, 5], and anthelmintic [6], with emphasis on their potential medicinal applications, is desirable. Here we are interested to study newly synthetized aminothiazoles, especially 2-aminothiazole derivatives which represent a class of heterocyclic ring system possessing antiviral [7], antimicrobial [8], anticancer [9], and anti-inflammatory activities [10]. Previously, in vitro anticancer evaluation studies of different 2-aminothiazole analogs exhibited their potent and selective nanomolar inhibitory activity against a wide range of human cancerous cell lines such as breast, leukemia, lung, colon, CNS, melanoma, ovarian, renal, and prostate cell lines [11–14]. Substitutions at 2-position benzothiazole have emerged in its usage as a core structure in the diversified therapeutic applications [15–21]. The studies of structure-activity relationship interestingly reveals that change of the structure of substituent group at C-2 position commonly results in the change of its bioactivity. Though literature survey reports many therapeutic applications of 2-substituted benzothiazoles, their investigation for anti-inflammatory activity is limited [16, 22–25]. Furthermore, thiazole derivatives have attracted a great deal of interest due to their wide applications in the field of pharmaceuticals. Thiazole derivatives display a wide range of biological activities such as cardiotonic, fungicidal, sedative, anesthetic, bactericidal, and anti-inflammatory [26, 27]. In addition, thiazole derivatives are reported to show a variety of biological activities. Depending on the substituents, this heterocycle possesses anthelmintic, antibiotic, and immunosuppressant activity [28]. Recent research indicates that some of 2-aminothiazoles derivatives are inhibitors of enzymes such as kynurenine-3-hydroxylase 29 or possess inhibitors activity against enzyme cyclin-dependent kinase [29].

Additionally, monoazo disperse dyes with thiazole-diazo components have been intensively investigated to produce bright and strong color shades ranging from red to greenish blue on synthetic fiber. Color Index described various basic, direct, vat, and disperse dyes wherein thiazole nucleus occurs [30]. Derivative of 2-aminothiazole has a long history of use as heterocyclic diazo components for disperse dyes [31].

In the present study, quantum chemical computations will be performed within DFT using WB97XD/6-31G(d) model to investigate the molecular structure, IR, and NMR of the newly synthetized molecules [32–38]. X-ray crystallographic data of 3B will be obtained and used to support

and verify the theoretical results. The energies of HOMO-LUMO frontier orbitals will be used to estimate molecular reactivation towards nucleophilic/electrophilic reagents. Electrostatic potential energy maps (ESP maps) will be graphically presented to locate binding sites of these new derivatives.

2. Experimental Section

2.1. Synthesis. All melting points were measured on an electric melting point apparatus and were uncorrected. The infrared spectra were recorded using potassium bromide disks on a Pye Unicam SP-3-300 infrared spectrophotometer; the established values of the gas phase frequencies are given between brackets. ^{1}HNMR spectra were run at 300 MHz, on a Varian Mercury VX-300 NMR spectrometer and Brukeravance III 400 MHZ, using TMS as an internal standard in deuterated dimethylsulphoxide. Chemical shifts δ are quoted in ppm. The mass spectra were recorded on Shimadzu GCMS-QP-1000EX mass spectrometers at 70 eV. All the spectral measurements were carried out at the NMR Laboratory of Cairo University, Egypt, and the NMR Laboratory of Faculty of Pharmacy, Ain shams University, Egypt; the microanalytical data were measured in Central Lab of Cairo University, Egypt; the Ministry of Defense Chemical Laboratories, Egypt; and the Microanalytical Center of Ain Shams University, Egypt. All the chemical reactions were monitored by TLC. The bold values corresponded to values calculated from DFT.

*2.1.1. General Procedure for the Preparation of Compounds **2a–g**.* A mixture of 2-aminothiazole **1** (1 g, 10 mmol) and different electrophilic reagents, namely, 2-chloro-N-(4-sulfamoylphenyl) acetamide, ethyl chloroacetate, phenyl cyanate, chloroacetyl chloride, 2-chloro-N-(4-chlorophenyl) acetamide, phenyl cyanate, phenyl thiocyanate, chloroacetyl chloride and 2-chloro-N-(4-chlorophenyl) acetamide (10 mmol) in dimethylformamide (20 ml), and anhydrous potassium carbonate, was refluxed for 5–8 h. The reaction mixture was poured in ice water (200 ml); the formed ppt was filtered off, dried, and crystallized from ethanol afforded compounds **2a**–**g**. It should be noticed that quantum chemically calculated spectroscopic parameters in gaseous phase are given in {bold font} for comparison with the experimentally obtained parameters.

*N-(4-Sulfamoylphenyl)-2-(thiazol-2-ylamino) Acetamide (**2a**).* Yield 65%; m.p. 118–120°C; orange crystals; (EtOH); IR (KBr) broad band at 3378, 3325, 3273 cm^{-1} (ν_{NH}), 3022 cm^{-1} ($\nu_{Aromatic}$), 2958 cm^{-1} ($\nu_{Aliphatic}$), 1691 cm^{-1} ($\nu_{C=O}$). ^{1}HNMR (300 MHz, DMSO-d$_6$) δ ppm: 5.1 (s, 2H, CH_2), 7.15 (d, 1H, thiazole H, J = 8.6 Hz), 7.4 (d, 1H, thiazole H, J = 8.6 Hz), 7.2 (s, 2H, NH_2, D_2O exchangeable), 7.7 (d, 2H, Ar-H), 7.8 (d, 2H, Ar-H), 10.8 (s, 1H, D_2O exchangeable NH), 7.1 and 12 (br s, 1H, D_2O exchangeable NH-OH tautomerism). Anal. Calculated for $C_{11}H_{12}N_4O_3S_2$ (312.36): C, 42.30; H, 3.87; N, 17.94 Found: C, 42.01; H, 4.07; N, 17.84.

*Ethyl thiazole-2-ylglycinate (**2b**).* Yield 80%; m.p. 142–144°C; orange crystals; (EtOH); IR (KBr) 3346 cm^{-1} (ν_{NH}), 3045 cm^{-1} ($\nu_{Olefinic}$), 1730 cm^{-1} ester ($\nu_{C=O}$). ^{1}HNMR (300 MHz, DMSO-d6) δ ppm: 1.4 (trip, 3H, CH3), 3.2 (quar, 2H, CH2), 5.1 (S, 2H, CH2), 7.0 (d, 1H, thiazole H, J = 8.4 Hz), 7.4 (d, 1H, thiazole H, J = 8.4 Hz), 10.2 (s, 1H, NH, D2O exchangeable), Anal. Calculated for $C_7H_{10}N_2O_2S$ (186.23): C, 45.15; H, 5.41; N, 15.04, Found: C, 45.01; H, 5.37; N, 14.84.

*1-Phenyl-3-(thiazole-2-yl) Urea (**2c**).* Yield 78%; m.p. 125–127°C; yellow crystals; (EtOH/benzene); IR (KBr) 3326, 3284 cm^{-1} (ν_{NH}), 3063 cm^{-1} ($\nu_{Aromatic}$), 1648 cm^{-1} ($\nu_{C=O}$). ^{1}HNMR (300 MHz, DMSO-d6) δ ppm: 7.00 (d, 2H, J = 7.2 HZ) 7.4 (m, 3H, ArH), 7.1 (d, 1H, thiazole H, J = 8.0 Hz), 7.8 (d, 1H, thiazole H, J = 8.0 Hz), 8.9 (s, 1H NH, D2O exchangeable,), 10.6 (s, 1H, NH, D2O exchangeable), ^{13}CNMR (300 MHz, DMSO-d6) δ ppm: 90.3, 100.2, 105.7, 120.8, 138.5, 140.9, 159.3, 165.4, Anal. Calculated for $C_{10}H_9N_3OS$ (219.26): C, 54.78; H, 4.14; N, 19.16, Found: C, 54.52; H, 4.17; N, 18.94.

*1-Phenyl-3-(thiazole-2-yl) Thiourea (**2d**).* Yield 76%; m.p. 178–180°C; brownish red crystals; (butanol); IR (KBr) 3169, 3081 cm^{-1} (ν_{NH}), 3009 cm^{-1} ($\nu_{aromatic}$). ^{1}HNMR (300 MHz, DMSO-d6) δ ppm: 7.00 (d, 2H, J = 7.2 HZ), 7.4 (m, 3H, ArH), 7.4 (d, 1H, thiazole H, J = 7.8 Hz), 7.6 (d, 1H, thiazole H, J = 7.8 Hz), 10.4 (s, 1H, NH, D_2O exchangeable), 12.4 (s, 1H, NH, D_2O exchangeable), ^{13}CNMR (300 MHz, DMSO-d6) δ ppm: 125.3, 126.4, 128.7, 129.4, 111.2, 137.4, 162.4, 176.6, Anal. Calculated for $C_{10}H_9N_3S_2$ (235.32): C, 51.04; H, 3.86; N, 17.86, Found: C, 51.01; H, 4.07; N, 17.74.

*2-Chloro-N-(thiazole-2-yl) Acetamide (**2e**).* Yield 60%; m.p. 220–222°C; brownish red crystals; m.p. 162–164°C (butanol); IR (KBr) 3187 cm^{-1} {*3643*} (ν_{NH}), 3041 cm^{-1} ($\nu_{olefinic\ H}$), 1703 cm^{-1} {*1825*} ($\nu_{C=O}$). ^{1}HNMR (300 MHz, DMSO-d6): δ ppm: 4.5 (s, 2H, CH2), 7.2 (d, 1H, thiazole H, J = 8.2 Hz), 7.6 (d, 1H, thiazole H, J = 8.2 Hz), 12.4 (s, 1H, NH, D_2O exchangeable), ^{13}CNMR (300 MHz, DMSO-d6) δ ppm: 39.7, 114.5, 137.7, 157.8, 157.6, 164.4, Anal. Calculated for $C_5H_5ClN_2OS$ (176.62): C, 34.00; H, 2.85; N, 15.86, Found: C, 34.12; H, 3.07; N, 15.74.

*N-(4-Chlorophenyl)-2-(thiazole-2-ylamino) Acetamide (**2f**).* Yield 68%; m.p. 198–200°C; red crystals; (butanol); IR (KBr) 3292, 3184 cm^{-1} (ν_{NH}), 3047 cm^{-1} ($\nu_{Aromatic}$), 1694 cm^{-1} ($\nu_{C=O}$). ^{1}HNMR (300 MHz, DMSO-d6) δ ppm: 2.4, 2.6 (s, 2H, 2NH, D2O exchangeable), 7.1 (s, 2H, CH_2), 7.2 (d, 2H, J = 7.6 Hz), 7.6 (m, 3H, ArH), 8.0 (d, 1H, thiazole H, J = 8.2 Hz), 8.2 (d, 1H, thiazole H, J = 8.2 Hz) Anal. Calculated for $C_{11}H_{10}ClN_3OS$ (267.73): C, 34.35; H, 3.76; N, 15.70, Found: C, 34.12; H, 3.67; N, 15.74.

*2.1.2. General Procedure for the Preparation of Compounds **3a–e**.* A mixture of **2e** (1.76 g, 10 mmol) and different nucleophilic reagents, namely, p-toluidine, thiourea, anthranilic, aminothiophenol, and quinoxaline-2,3-diol (10 mmol) in dimethylformamide (20 ml) and anhydrous potassium carbonate was refluxed for 4-5 h. The reaction mixture was

poured onto ice water (200 ml). The formed precipitate was filtered off and recrystallized from the suitable solvent to afford compounds 3a–e.

*3-(Thiazole-2-ylamino) Benzo[e][1,4]oxazepin-5(1H)-one (**3a**)*. Recrystallized from ethanol to produce brownish red crystals, Yield 84%; m.p. 252–254°C; (butanol); IR (KBr) 3672, 3377 cm^{-1} {*3677 asym, 3680 sym*} (ν_{NH}), 3198 cm^{-1} {*3267 asym str*} ($\nu_{H\ of\ thiazole}$), 3020 cm^{-1} ($\nu_{Aromatic}$), 2967.42 cm^{-1} {*3095 sym str*} (ν_{CH2}) 1698 cm^{-1} ($\nu_{C=O}$). ^{1}HNMR (300 MHz, DMSO-d6) δ ppm: 7.2 (d, 1H, thiazole H, J = 8.2 Hz), 7.4 (d, 1H, thiazole H, J = 8.2 Hz), 7.6 (d, 2H, ArH, J = 8.1 Hz), 7.8 (m, 2H, ArH), 8.2 (s, 1H, NH, D_2O exchangeable), 8.8 (s, 1H, 1-ethelyene), 11.4 (s, 1H, NH, D_2O exchangeable), Anal. Calculated for $C_{12}H_9N_3O_2S$ (259.28): C, 55.59; H, 3.50; N, 16.21, Found: C, 55.45; H, 3.67; N, 16.14.

*N-(Thiazole-2-yl)-2-(p-tolylamino) Acetamide (**3b**)*. Oily product, solidified with diethyl ether, Yield 44%; m.p. 235–237°C; brownish red crystals; (butanol); IR (KBr) 3287, 3150 cm^{-1} (ν_{NH}), 3045 cm^{-1} ($\nu_{Aromatic}$), 1701 cm^{-1} ($\nu_{C=O}$). ^{1}HNMR (300 MHz, DMSO-d6) δ ppm: 2.11 (s, 3H, CH3), 3.5 (s, 2H CH2), 6.25 (**6.32**) (d, 2H, Ar benz, J = 6.8 Hz), **6.41** (**6.52**) (d, 1H, thiazole H, J = 8.2 Hz), 7.0 (**7.1**) (d, 2H, ArH, J = 8.1 Hz), 7.3 (**7.4**) (d, 1H, thiazole H, J = 8.2 Hz), 8.01 (**7.8**) (d, 2H, ArH, J = 6.8 Hz), 11.4 (s, 1H, NH, D_2O exchangeable), Anal. Calculated for $C_{12}H_{13}N_3OS$ (247.32): C, 58.28; H, 5.30; N, 16.99, Found: C, 58.45; H, 5.67; N, 16.80.

*4-(Thiazole-2-ylamino)-1,5-dihydro-2H-imidazole-2-thione (**3c**)*. Dried and crystallized from ethanol the product has brownish red crystals; m.p. 206–208°C; Yield 54%; (butanol); IR (KBr) 3374, 3275 cm^{-1} (ν_{NH}), 3045 cm^{-1} ($\nu_{Aromatic}$), 2600 cm^{-1} (ν_{SH}), 1260 cm^{-1} ($\nu_{C=S}$), ^{1}HNMR (300 MHz, DMSO-d6) δ ppm: 4.22 (s, 2H, imidazole H), 6.9 (d, 1H, thiazole H, J = 7.4 Hz), 77.2 (d, 1H, thiazole H, J = 7.4 Hz), 9.5 (s, H, NH, D_2O exchangeable), 13.2 (s, H, imidazole NH, D_2O exchangeable), Anal. Calculated for $C_6H_6N_4S_2$ (198.00): C, 36.35; H, 3.05; N, 28.26 Found: C, 36.45; H, 3.25; N, 28.32.

*N-(Thiazole-2-yl)-4H-benzo[b][1,4]thiazine-2-amine (**3d**)*. Dried and crystallized from butanol, Yield 62%; brownish red crystals; m.p. 262–266°C; (butanol); IR (KBr) 3445.47, 3310.31 cm^{-1} {*3713 str, hetero ring, 3680 str, link NH*} (ν_{NH}), 3198.45 cm^{-1} {*3247*} ($\nu_{CH\ ring}$), 3063 cm^{-1} ($\nu_{Aromatic}$), 1663.89 cm^{-1} {*1639*} ($\nu_{C=N\ triazol}$), ^{1}HNMR (300 MHz, DMSO-d6) δ ppm: 5.1 (s, H, Thiazine H), 7.0 (d, 2H, ArH, J = 7.9 Hz), 7.4 (m, 2H, ArH), 7.5 (d, 1H, thiazole H, J = 8.2 Hz), 7.6 (d, 1H, thiazole H, J = 8.2 Hz), 10.8, 12.2 (s, 2H, 2NH, D2O exchangeable), ^{13}CNMR (300 MHz, DMSO-d6) δ ppm: 114.6, 122.2, 123.7, 124.6, 126.8, 141.0, 153.6, 155.7, 165.4, Anal. Calculated for $C_{11}H_9N_3S_2$ (247.33): C, 53.42; H, 3.67; N, 16.99, Found: C, 36.45; H, 3.25; N, 28.32.

*2-((3-Hydroxyquinoxalin-2-yl)oxy)-N-(thiazole-2-yl) Acetamide (**3e**)*. Crystallized from ethanol, Yield 58%; m.p. 298–300°C; brownish red crystals; (butanol); IR (KBr) broad band at 3450 cm^{-1} {*3787 of hetero ring*} (ν_{OH}), 3342 cm^{-1} {*3643 of hetero ring*} (ν_{NH}), 3190 cm^{-1} {*3256*} ($\nu_{CH\ of\ hetero\ ring}$), 3120 cm^{-1} {*3107*} (ν_{CH2}), 3048 cm^{-1} ($\nu_{Aromatic}$), 1725 cm^{-1} {*1834*} ($\nu_{C=O}$), 1658 cm^{-1} ($\nu_{C=N}$). ^{1}HNMR (300 MHz, DMSO-d6) δ ppm: 5.4 (s, 2H, CH2), 7.4 (s, 1H, NH, D_2O exchangeable), 7.5 (d, 2H, ArH, J = 8.2 Hz), 7.7 (m, 2H, ArH), 8.0 (d, 1H, thiazole H, J = 8.56 Hz), 8.2 (d, 1H, thiazole H, J = 8.56 Hz), 13.2 (s, 1H, OH, D_2O exchangeable), Anal. Calculated for $C_{13}H_{10}N_4O_3S$ (302.31): C, 51.65; H, 3.33; N, 18.53, Found: C, 51.56; H, 3.21; N, 18.56.

2.2. X-Ray Crystallography. X-ray structure analysis offers perfect addition to our synthetic work. X-ray structures of the compound 3b were performed in the Central Service and X-Ray Laboratories, National Research Centre, Cairo, Egypt. Crystal and molecular structures were prepared by Maxus Computer Program for the Solution and Refinement of Crystal Structures. All diagrams and calculations were performed using maXus (Bruker Nonius, Delft; MacScience, Japan). There was no extinction correction. Atomic scattering factors were from Waasmaier and Kirfel, 1995. Data collection parameters are as follows: KappaCCD; cell refinement: HKL Scalepack; data reduction: Denzo Program(s) used to solve structure; SIR92 and Scalepak Program(s) used to refine structure; maXus: ORTEP Software which was used for molecular graphics. Crystal data, fractional atomic coordinates, and equivalent isotropic thermal parameters, anisotropic displacement parameters and geometric parameters of compounds 3b are given in Table 2. The additional data for the molecule 3b are alternatively available from the Cambridge Crystallographic Data Centre as CCDC1402910.

2.3. Computations. Computations were carried out using Gaussian 16 revision A.03 package [32] and/or Spartan'16 parallel QC program [Wavefunction, Inc., USA]. Optimized structures and spectroscopic data derived from quantum chemical calculations have been used within the WB97DX/6-31G(d) model. A Broadberry (UK) 40-core workstation and/or MAC Pro 12-core computers were used.

3. Result and Discussion

3.1. Synthesis and Spectroscopic Properties. In our study, 2-aminothiazole 1 was used as a key starting material. Reaction of 1 with chloro-N-(4-sulfamoylphenyl) acetamide afforded the amide derivative 2a (Scheme 1). The structure of 2a is substantiated from its spectral data. The IR spectrum shows appearance of absorption band of C=O group for the amide at 1691 cm^{-1}, as well as the presence of OH-NH tautomerization at δ 7.1 ppm and 12 ppm. On the other hand, when 1 was refluxed in dimethylformamide with ethyl chloroacetate, the ester 2b was abstained and its structure was confirmed with different spectral data: the presence of the ester C=O at 1730 cm^{-1} in IR, for example, and the presence of CH_2CH_3 in H-NMR as quartet and triplet at δ 3.2, 1.4 ppm, respectively.

In addition, urea and thiourea derivatives 2c, 2d were obtained from the reaction of the aminothiazole with phenyl isocyanate and phenyl isothiocyanate. The IR spectrum revealed the absence of doublet bands of NH_2 in both compounds, the appearance of band that is attributed to

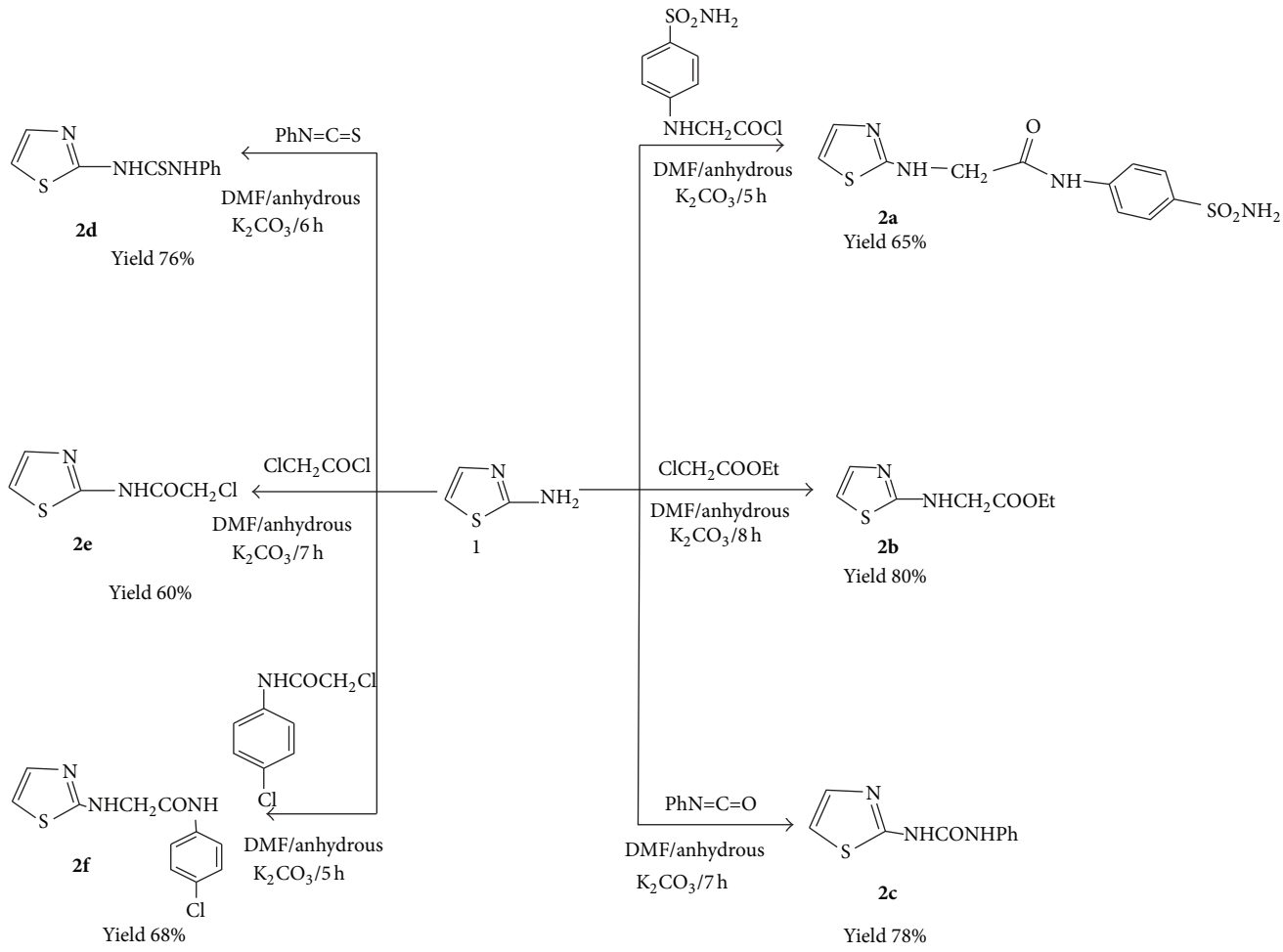

Scheme 1

C=O for 2c at 1648 cm^{-1}, and the appearance of four peaks that is attributed to phenyl ring in C^{13}-NMR. The most important compound in this work is compound 2e that resulted from interaction of 1 with chloroacetyl chloride; the structure was proved by appearance of C=O at 1703 cm^{-1} as well as absence of NH_2 doublets. The amide derivative 2f is obtained from reaction of thiazole derivative with 2-chloro-N-(4-chlorophenyl) acetamide; the IR spectrum shows the presence of C=O band and the presence of double doublets of para-substituted-benzene ring of chlorophenyl in H-NMR.

The compound 2e was the key start for many other reactions; refluxing 2e with anthranilic acid afforded the oxazipin-one 3a (Scheme 2). The cyclic structure was proved from IR spectrum which showed the absence of broad OH band that is attributed to open structure and the appearance of C=O band at 1698 cm^{-1}.

On the other hand, the amide derivatives 3b were obtained from reaction of 2e with p-toluidine for five hours; the open structure was confirmed with many tools as IR which show two NH bands at 3287, 3150 cm^{-1}, as well as the X-Ray crystallography; furthermore, refluxing of chloroderivative 2e with thiourea afforded cyclic structure 3c, which had been proved with absence of C=O band in IR and appearance of 3374 and 3275 cm^{-1} for 2 NH. Furthermore, the appearance of weak band as 2600 cm^{-1} is attributed to thione-thiol SH tautomerization. The thiazine 3d is another cyclic compound resulting from refluxing 2e with 2-aminophenol; the structure was proved by disappearance of C=O, as well as the appearance of peak in H-NMR for thiazine H at δ 5.1 ppm and appearance for extra peak at δ 114 ppm for thiazine ring in C^{13}-NMR.

At last, refluxing 2e with quinoxaline-2,3-diol in DMF/anhydrous carbonate produced the ether 3e, whose structure was evaluated from IR by peaks at 1725 cm^{-1} for C=O, appearance of broad band at 3350 cm^{-1} that is attributed to OH, and, in addition, aromatic peaks in H-NMR at δ 7.5 ppm and 7.7 ppm.

3.2. X-Ray Crystallography and Optimized Molecular Structure. X-ray results are depicted in Table 1. X-ray structure analysis offers perfect addition to our synthetic work. X-ray structures of the compound 3b (Figure 1) showed that the molecule is planar. Table 2 shows the agreement between the optimized parameters and the experimentally obtained geometry of 3B molecule.

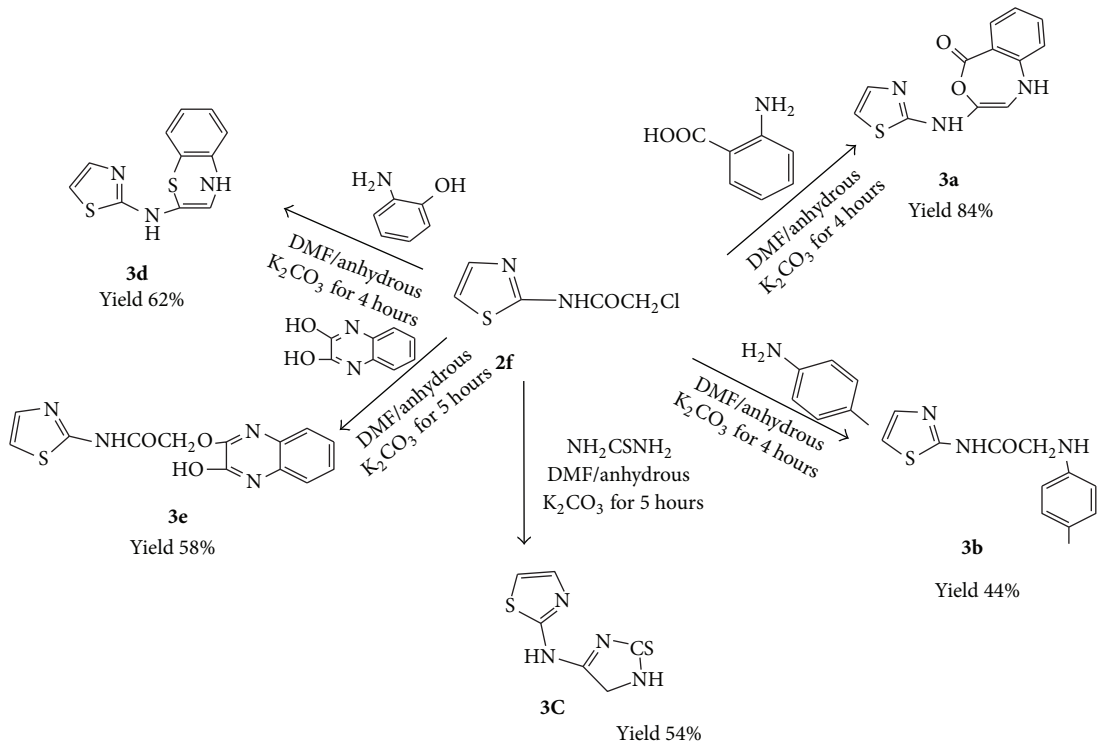

Scheme 2

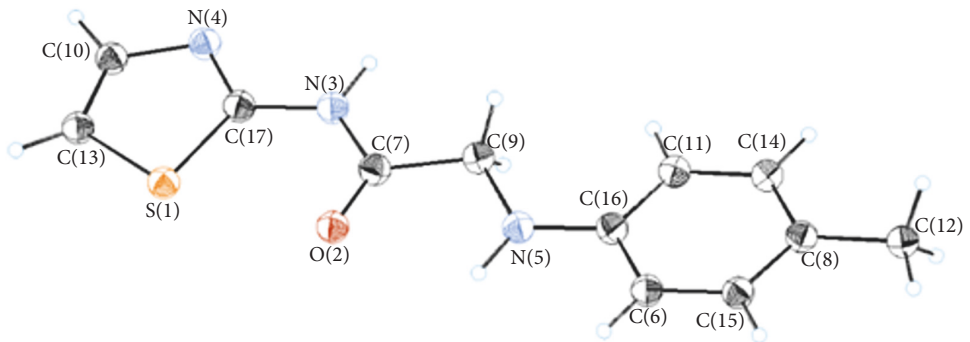

Figure 1: X-ray crystallographic drawing of molecule **3b**.

The structure produced (Figure 1 and Table 2) is in excellent match with the optimized structure obtained by quantum chemical calculations within the density functional theory (DFT) [33, 34] using WB97XD/6-31G(d) model.

3.3. Molecular Reactivities. Chemical reactivity theory quantifies the reactive propensity of isolated species through the introduction of a set of reactivity indices or descriptors. Its roots go deep into the history of chemistry, as far back as the introduction of such fundamental concepts as acid, base, Lewis acid, and Lewis base. It pervades almost all of chemistry.

The most relevant indices defined within the conceptual DFT [33] for the study of the organic reactivity are discussed elsewhere [35–39]. *Molecular reactivity indices [35–39] such as chemical potential ($\boldsymbol{\mu}$), hardness ($\boldsymbol{\eta}$), and electrophilicity ($\boldsymbol{\omega}$) were computed from the energies of frontier orbitals and defined as follows:*

(1) *Chemical potential is given by*

$$\boldsymbol{\mu} \approx -\frac{1}{2}(I + A) \approx \frac{1}{2}(\epsilon_L - \epsilon_H) \quad (1)$$

or simply $\boldsymbol{\mu} = \mathbf{0.5}$(LUMO + HOMO).

(2) *Hardness is given by*

$$\boldsymbol{\eta} \approx \frac{1}{2}(I - A) \approx \frac{1}{2}(\epsilon_L - \epsilon_H) \quad (2)$$

or simply $\boldsymbol{\eta} = \mathbf{0.5}$(LUMO − HOMO). The chemical hardness $\boldsymbol{\eta}$ can be thought as a resistance of

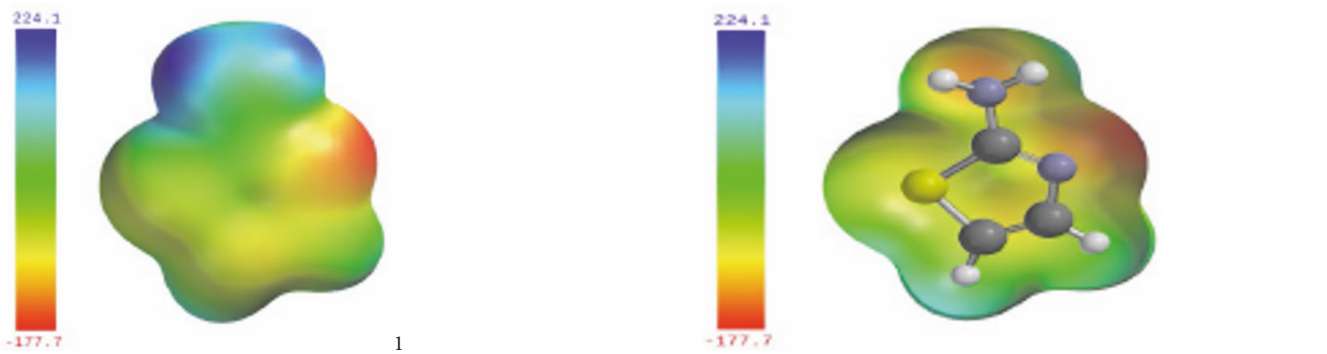

1

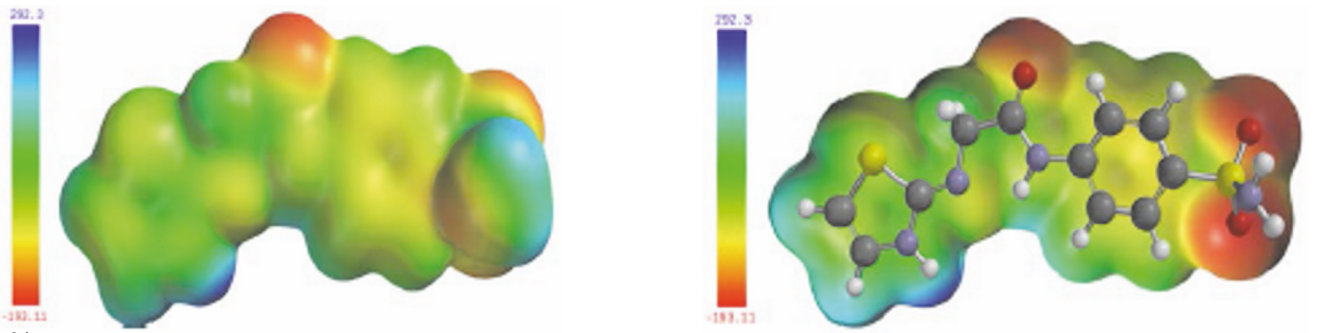

2A

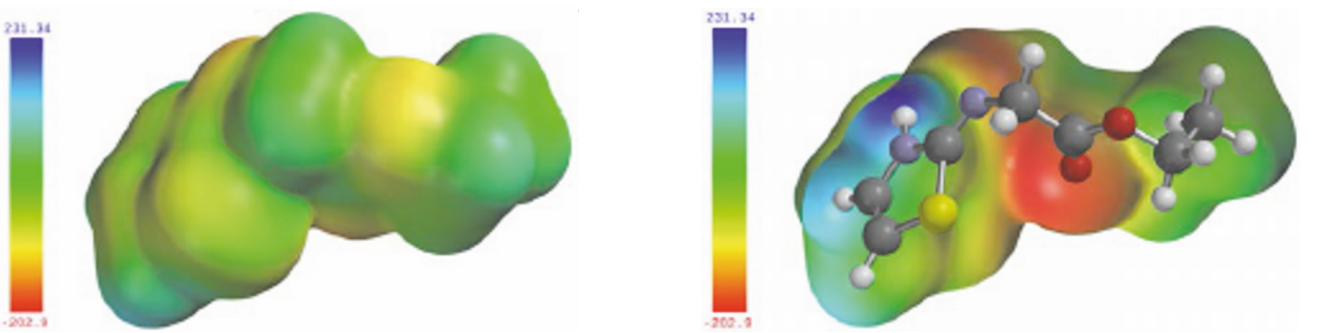

2B

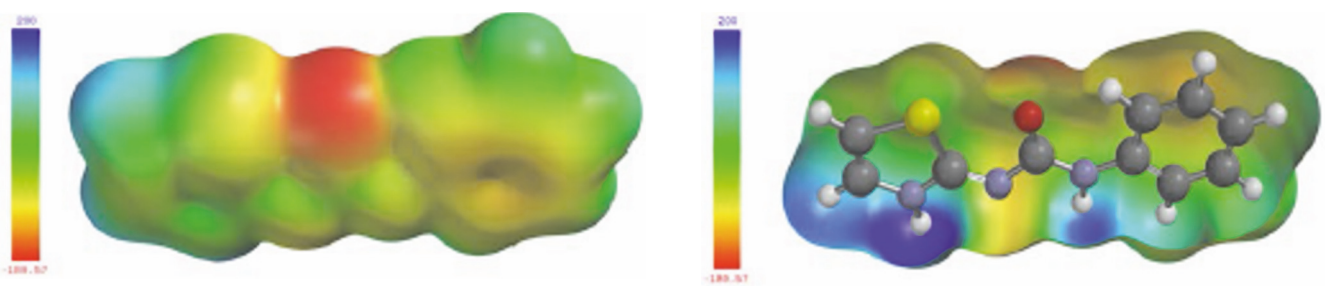

2C

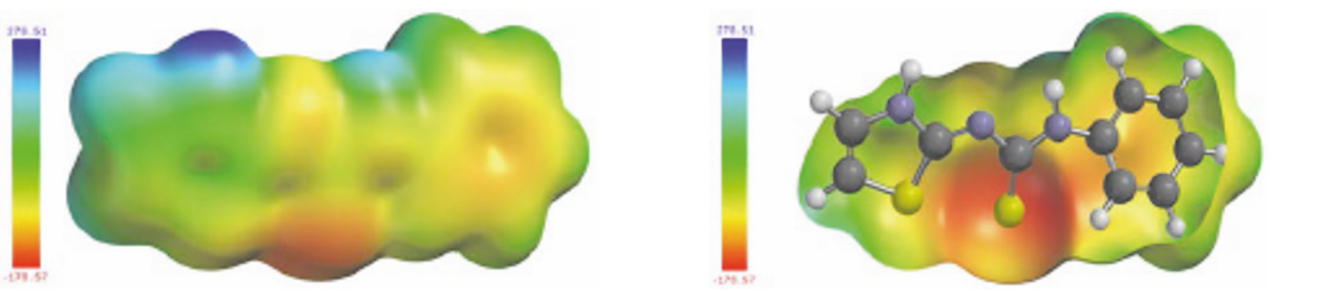

2D

Figure 2: Continued.

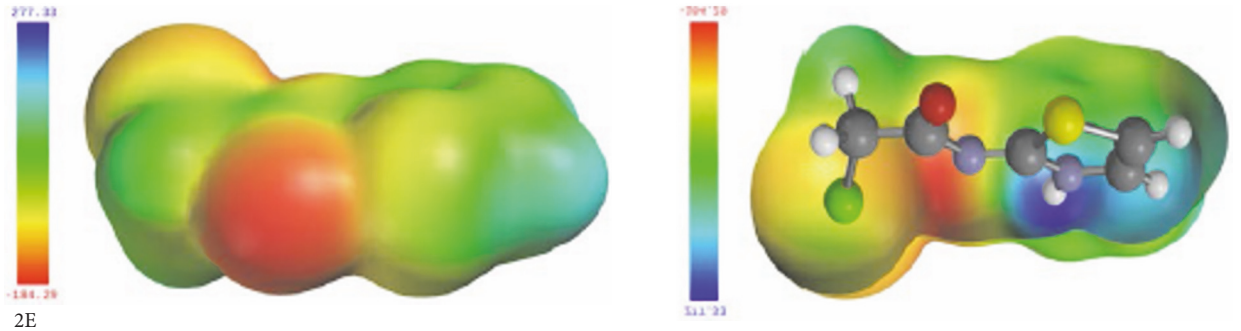

2E

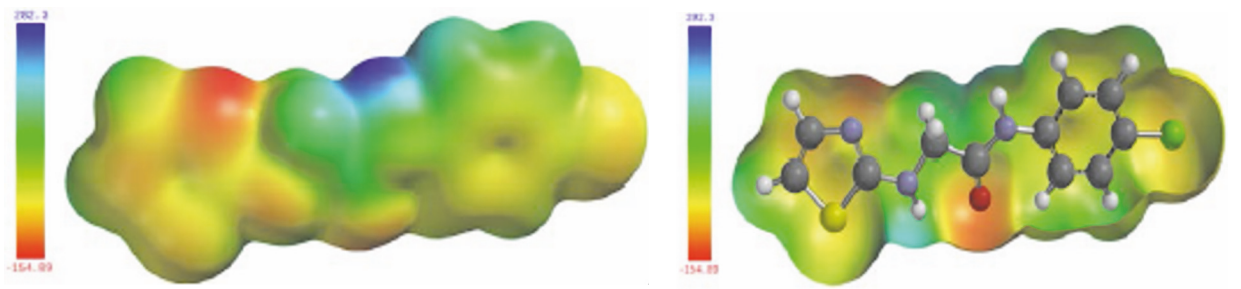

2F

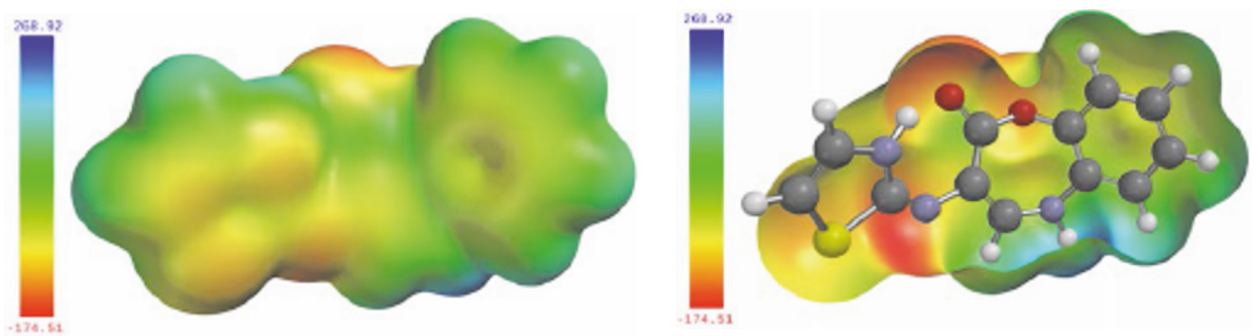

3A

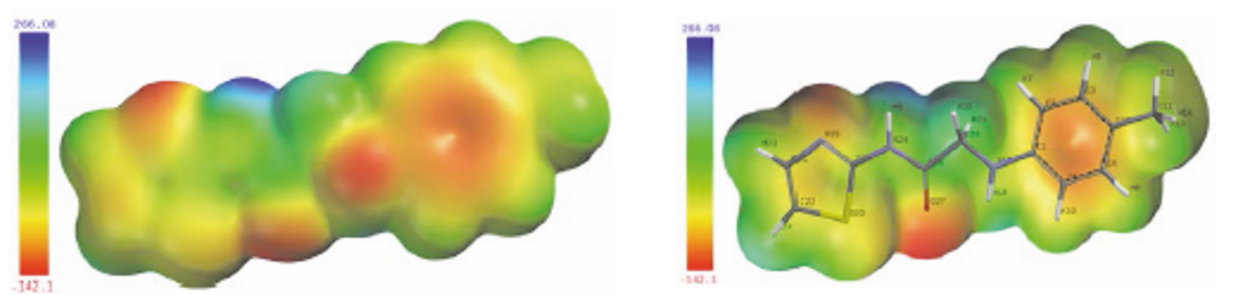

3B

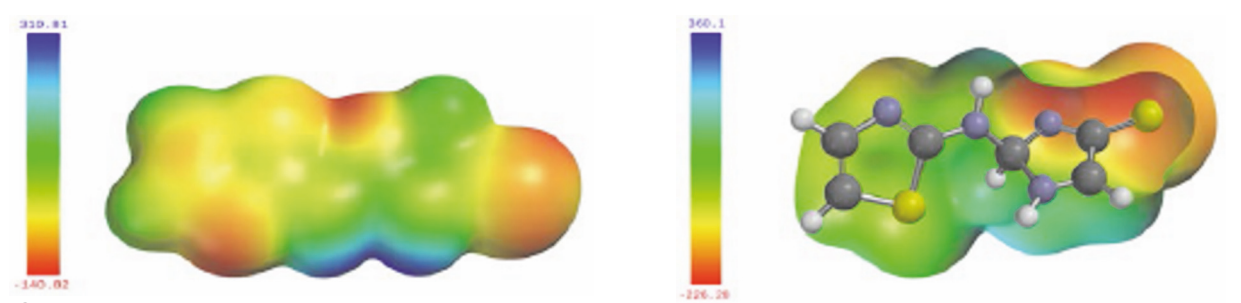

3C

Figure 2: Continued.

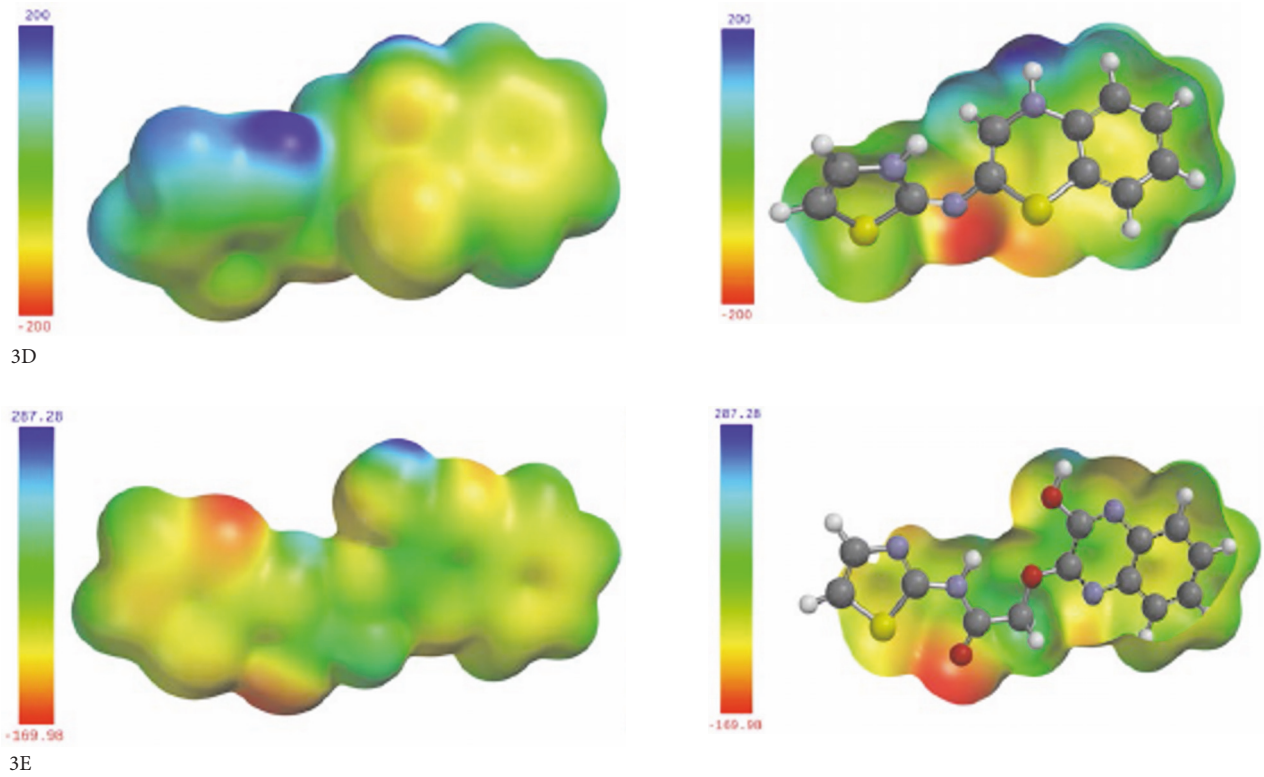

FIGURE 2: ESP maps (solid surface at left side and clipped surfaces at the right side showing atoms). The results should improve our knowledge about the binding sites, which are of importance in medical applications. Color code bars reflect electrostatic potential energy values in kJ/mol. The redder the area is, the higher the electron density is susceptible to nucleophilic attack and the bluer the area is, the lower the electron density is that could easily binds with an electrophile.

TABLE 1: Crystal experimental data for compound **3b**.

Parameter	Results
Empirical formula	$C_{12}H_{13}N_3OS$
Formula weight (g mol^{-1})	M_r = 247.08
Temperature	T = 298 K
Crystal system	Monoclinic
Space group	$P2_1/c$
a (Å)	15.1986 (6)
b Å	5.2675 (2)
c Å	20.1741 (10)
α (deg)	90.00°
β (deg)	110.478 (2)°
γ (deg)	90.00°
V Å^3	1513.04 (11)
Z	4
D_x:	1.288 Mg m^{-3}
Radiation	Mo $K\alpha$ (λ = 0.71073)
μ (mm^{-1})	0.22
Color	Colorless

a molecule to exchange electron density with the environment.

(3) *Electrophilicity:* in 1999, Parr defined the electrophilicity index [40] $\boldsymbol{\omega} = \boldsymbol{\mu}^2/2\eta$, which *measures the total ability to attract electrons*. The electrophilicity index gives a measure of the energy stabilization of a molecule when it acquires an additional amount of electron density from the environment. The electrophilicity index comprises the tendency of an electrophile to acquire an extra amount of electron density, given by $\boldsymbol{\mu}$ and the resistance of a molecule to exchange electron density with the environment, given by $\boldsymbol{\eta}$. Therefore, a good electrophile is a species characterized by a high absolute $\boldsymbol{\mu}$ value and a low $\boldsymbol{\eta}$ value. The electrophilicity index has become a powerful tool for the study of the reactivity of organic molecules [36].

(4) *Nucleophilicity (N):* while the electrophilicity of the molecules accounts for the reactivity towards nucleophiles, it has been shown by Domingo and his coworkers [36–39] that a simple index chosen for the nucleophilicity, N, based on the HOMO energy, within DFT, is useful to explain the reactivity of these new compounds towards electrophiles.

Nucleophilicity index is defined as $N = E_{\mathrm{HOMO}}$ (eV) + 9.12 (eV), where -9.12 is the energy of the HOMO of tetracyanoethylene (TCE).

It is noteworthy to mention that this nucleophilicity scale is referred to tetracyanoethylene (TCE) taken as

Table 2: Geometric parameters (Å, °).

Bonds and angles	X-ray	Modeled
S1-C13	1.721 (4)	1.7997
S1-C17	1.707 (4)	1.8053
O2-C7	1.214 (4)	1.2438
N3-C7	1.369 (5)	1.3731
N3-C17	1.382 (4)	1.3864
N4-C17	1.309 (4)	1.3014
N4-C10	1.379 (5)	1.4034
N5-C16	1.391 (4)	1.3853
N5-C9	1.437 (4)	1.4389
C6-C15	1.355 (5)	1.386
C6-C16	1.397 (5)	1.4087
C7-C9	1.519 (5)	1.5211
C8-C14	1.381 (5)	1.3928
C8-C15	1.384 (5)	1.403
C8-C12	1.508 (5)	1.5147
C10-C13	1.321 (5)	1.3513
C11-C14	1.378 (5)	1.3967
C11-C16	1.385 (5)	1.4023
N3-H3	0.9598	1.0171
N5-H5	0.9600	1.0139
C6-H6	0.9600	1.0861
C9-H9A	0.9599	1.103
C9-H9B	0.9600	1.103
C10-H10	0.9601	1.0787
C11-H11	0.9602	1.0845
C12-H12A	0.9600	1.0946
C12-H12B	0.9600	1.0963
C12-H12C	0.9600	1.0963
C13-H13	0.9600	1.0777
C14-H14	0.9602	1.0865
C15-H15	0.9601	1.0867
C13-S1-C17	87.9 (2)	86.3009
C7-N3-C17	123.7 (3)	125.9603
C17-N4-C10	108.1 (3)	111.3904
C16-N5-C9	121.1 (3)	122.897
C15-C6-C16	120.3 (4)	120.6207
O2-C7-N3	122.8 (4)	122.4876
O2-C7-C9	124.6 (4)	123.1669
N3-C7-C9	112.6 (4)	114.3456
C14-C8-C15	116.2 (4)	117.6113
C14-C8-C12	121.8 (4)	121.8524
C15-C8-C12	121.9 (4)	120.5363
N5-C9-C7	109.7 (3)	108.4
C13-C10-N4	116.7 (4)	115.7669
C14-C11-C16	121.4 (4)	119.8642
C10-C13-S1	110.6 (3)	111.058
C8-C14-C11	121.5 (4)	121.6167
C6-C15-C8	123.3 (4)	121.5706
C11-C16-N5	123.5 (4)	122.0228
C11-C16-C6	117.1 (4)	118.1129
N5-C16-C6	119.4 (4)	119.8642
N4-C17-N3	119.5 (3)	121.0122
N4-C17-S1	116.6 (3)	115.4839
N3-C17-S1	123.9 (3)	123.504
C7-N3-H3	119.5	120.0392
C17-N3-H3	116.8	114.0005
C16-N5-H5	120.7	120.8726
C9-N5-H5	118.2	116.2304
C15-C6-H6	122.1	119.9912
C16-C6-H6	117.5	119.3881
N5-C9-H9A	108.9	119.3881
C7-C9-H9A	110.6	108.6962
N5-C9-H9B	108.2	111.6719
C7-C9-H9B	109.9	108.6961
H9A-C9-H9B	109.5	107.5286
C13-C10-H10	124.8	126.0377
N4-C10-H10	118.4	118.1954
C14-C11-H11	119.2	118.9467
C16-C11-H11	119.4	120.5856
C8-C12-H12A	109.8	110.988
C8-C12-H12B	109.1	110.9831
H12A-C12-H12B	109.5	107.9859
C8-C12-H12C	109.5	110.9833
H12A-C12-H12C	109.5	107.7767
H12B-C12-H12C	109.5	107.9859
C10-C13-H13	129.4	128.4417
S1-C13-H13	120.0	120.5003
C8-C14-H14	119.0	119.5425
C11-C14-H14	119.5	118.8408
C6-C15-H15	117.9	119.1455
C8-C15-H15	118.8	119.2839

a reference, because it presents the lowest HOMO energy in a large series of molecules investigated [36].

The numerical parameters reflect the tendency of transferring electronic charges during chemical interactions between molecules (Table 3). Electrophilicity is an important reactivity descriptor that is considered as a measure of a compound's willingness to participate as an electron acceptor during a chemical reaction, or, in other words, the electron deficiency of a compound. 3E is the molecule with the largest electrophilicity $\boldsymbol{\omega}$, whereas 3D is the one showing smallest electrophilicity indicating lower susceptibility towards nucleophilic reaction. Table 3 shows that chemical potential value, which is the negative of molecular electronegativity reflecting the escaping tendency of electrons, decreases in the following order: 3D > 2B > 3B > 2C > 3A > 2F > 2D > 2E > 2A > 3C > 3E.

By examining the nucleophilicity descriptor N (Table 3) for these molecules, we found that 2E ($N = 0.78$ eV) is one of the poorest nucleophiles of this series, while 3D ($N = 2.97$ eV) represents the best nucleophile. Generally, nucleophilicity increases in the following order: 2E < 2A < 3C < 3E < 2C < 2B < 2F < 2D < 3B < 3A < 3D

These results are consistent with the expected reactivity pattern.

Table 3: Reactivity indices* sorted according to ascending electrophilicity ω.

Molecule	HOMO	LUMO	μ	η	ω	N
1	−7.78	1.90	−2.94	4.84	0.64	1.34
3D	−6.15	1.31	−2.42	3.73	0.79	2.97
2B	−7.61	1.99	−2.81	4.55	0.87	1.51
2C	−7.80	1.28	−3.26	4.54	1.17	1.32
3B	−7.20	0.97	−3.12	4.09	1.19	1.92
2F	−7.61	1.04	−3.29	4.33	1.25	1.51
3A	−6.96	0.59	−3.19	3.78	1.34	2.16
2D	−7.42	0.53	−3.45	3.98	1.49	1.70
2E	−8.34	0.91	−3.72	4.63	1.50	0.78
2A	−8.31	0.73	−3.79	4.52	1.59	0.81
3C	−8.19	0.29	−3.95	4.24	1.84	0.93
3E	−8.11	0.08	−4.02	4.10	1.97	1.01

*HOMO, LUMO, μ, η, and N are in eV.

Investigation of a molecule's surface is probably a good start for considerations of the molecule's reactivity since this is where two approaching molecules would first interact. ESP maps are depicted in Figure 2. The results should improve our knowledge about the binding sites, which are of importance in chemical reactivities and medical applications. Color codes point to the binding sites when interacting with other reagents [41–43] (see caption of Figure 2).

4. Conclusions

One-step syntheses of 12 thiazole derivatives of medicinal importance are performed. Optimized structures, reactivity indices, electrostatic potential energy maps, and spectroscopic properties such as IR and NMR of the newly reported molecules are computed within DFT using WB97XD/6-31G(d) model. Satisfactory agreement between experiment and theory is observed. Trends in chemical reactivities are investigated. Molecules 3E and 3D have the largest and smallest electrophilicity, respectively. Generally, based on relative nucleophilicity index N, nucleophilicity increases in the following order: 2E < 2A < 3C < 3E < 2C < 2B < 2F < 2D < 3B < 3A < 3D. These results are consistent with the expected reactivity pattern.

The graphically visualized ESP maps enable locating the binding sites of these molecules.

Conflicts of Interest

The authors declare that they have no conflicts of interest.

References

[1] C. H. Oh, H. W. Cho, D. Baek, and J. H. Cho, "Synthesis and antibacterial activity of 1β-methyl-2-(5-substituted thiazole pyrrolidin-3-ylthio) carbapenem derivatives," *European Journal of Medicinal Chemistry*, vol. 37, pp. 743–754, 2002.

[2] R. A. Tapia, Y. Prieto, F. Pautet et al., "Synthesis and antiprotozoal evaluation of benzothiazolopyrroloquinoxalinones, analogues of kuanoniamine A," *Bioorganic and Medicinal Chemistry*, vol. 11, no. 16, pp. 3407–3412, 2003.

[3] G. V. Suresh Kumar, Y. Rajendraprasad, B. P. Mallikarjuna, S. M. Chandrashekar, and C. Kistayya, "Synthesis of some novel 2-substituted-5-[isopropylthiazole] clubbed 1,2,4-triazole and 1,3,4-oxadiazoles as potential antimicrobial and antitubercular agents," *European Journal of Medicinal Chemistry*, vol. 45, no. 5, pp. 2063–2074, 2010.

[4] P. Samadhiya, R. Sharma, S. K. Srivastava, and S. D. Srivastava, "Synthesis of 2-oxoazetidine derivatives of 2-aminothiazole and their biological activity," *Journal of the Serbian Chemical Society*, vol. 77, no. 5, pp. 599–605, 2012.

[5] S. K. Sonwane and S. D. Srivastava, "Synthesis and biological significance of 2-amino-4-phenyl-1,3-thiazole derivatives," *Proceedings of the National Academy of Sciences, India*, vol. 78, no. 2, pp. 129–136, 2008.

[6] S. K. Srivastava, R. Yadav, and S. D. Srivastava, "Synthesis and biological activity of 4-oxothiazolidines and their 5-arylidenes," *Indian Journal of Chemistry*, vol. 43B, no. 2, pp. 399–405, 2004.

[7] S. Ghaemmaghami, B. C. H. May, A. R. Renslo, and S. B. Prusiner, "Discovery of 2-aminothiazoles as potent antiprion compounds," *Journal of Virology*, vol. 84, no. 7, pp. 3408–3412, 2010.

[8] H. L. Siddiqui, M. Zia-Ur-Rehman, N. Ahmad, G. W. Weaver, and P. D. Lucas, "Synthesis and antibacterial activity of bis[2-amino-4-phenyl-5-thiazolyl] disulfides," *Chemical and Pharmaceutical Bulletin*, vol. 55, no. 7, pp. 1014–1017, 2007.

[9] E. A. Kesicki, M. A. Bailey, Y. Ovechkina et al., "Synthesis and evaluation of the 2-aminothiazoles as anti-tubercular agents," *PLOS ONE*, vol. 11, no. 5, 2016.

[10] P. Lin, R. Hou, H. Wang, I. Kang, and L. Chen, "Efficient Synthesis of 2-Aminothiazoles and Fanetizole in Liquid PEG-400 at Ambient Conditions," *Journal of the Chinese Chemical Society*, vol. 56, no. 3, pp. 455–458, 2009.

[11] M. J. Gorczynski, R. M. Leal, S. L. Mooberry, J. H. Bushweller, and M. L. Brown, "Synthesis and evaluation of substituted 4-aryloxy- and 4-arylsulfanyl- phenyl-2-aminothiazoles

as inhibitors of human breast cancer cell proliferation," *Bioorganic and Medicinal Chemistry*, vol. 12, no. 5, pp. 1029–1036, 2004.

[12] R. N. Misra, H.-Y. Xiao, D. K. Williams et al., "Synthesis and biological activity of N-aryl-2-aminothiazoles: potent pan inhibitors of cyclin-dependent kinases," *Bioorganic and Medicinal Chemistry Letters*, vol. 14, no. 11, pp. 2973–2977, 2004.

[13] H. I. El-Subbagh, A. H. Abadi, and J. Lehmann, "Synthesis and Antitumor Activity of Ethyl 2-Substituted-aminothiazole-4-carboxylate Analogs," *Archiv der Pharmazie*, vol. 332, no. 4, pp. 137–142, 1999.

[14] I. Kayagil and S. Demirayak, "Synthesis and anticancer activities of some thiazole derivatives," *Phosphorus, Sulfur and Silicon and the Related Elements*, vol. 184, no. 9, pp. 2197–2207, 2009.

[15] Priyanka, K. S. Neeraj, and K. J. Keshari, "Benzothiazole: the molecule of diverse biological activities," *International Journal of Current Pharmaceutical Research*, vol. 2, p. 1, 2010.

[16] H. P. Singh, C. S. Sharma, and C. P. Gautam, "Synthesis and pharmacological screening of some novel 2-arylhydrazino and 2-aryloxy-pyrimido [2,1-b] benzothiazole derivatives," *American-Eurasian Journal of Scientific Research*, vol. 4, no. 4, pp. 222–228, 2009.

[17] H. Kaur, S. Kumar, I. Singh, K. K. Saxena, and A. Kumar, "Synthesis, characterization and biological activity of various substituted benzothiazole derivatives," *Digest Journal of Nanomaterials & Biostructures*, vol. 5, no. 1, pp. 67–76, 2010.

[18] A. A. Chavan and N. R. Pai, "Synthesis and biological activity of N-substituted-3-chloro-2-azetidinones," *Molecules*, vol. 12, no. 11, pp. 2467–2477, 2007.

[19] S. Nadeem, R. Arpana, A. K. Suroor et al., "Synthesis and preliminary screening of benzothiazol-2-yl thiadiazole derivatives for anticonvulsant activity," *Acta Pharmaceutica*, vol. 59, no. 4, pp. 441–451, 2009.

[20] N. A. Masoudi, W. Pfleiderer, and C. Pannecouque, "Nitroimidazoles part 7. synthesis and anti-HIV activity of new 4-nitroimidazole derivatives," *Zeitschrift für Naturforschung B*, vol. 67, no. 8, pp. 835–842, 2014.

[21] P. Gajdoš, P. Magdolen, P. Zahradník, and P. Foltínová, "New conjugated benzothiazole-N-oxides: synthesis and biological activity," *Molecules*, vol. 14, no. 12, pp. 5382–5388, 2009.

[22] R. K. Gill, R. K. Rawal, and J. Bariwal, "Recent advances in the chemistry and biology of benzothiazoles," *Archiv der Pharmazie*, vol. 348, no. 3, pp. 155–178, 2015.

[23] R. Paramashivappa, P. Phani Kumar, P. V. Subba Rao, and A. Srinivasa Rao, *Bioorg.Med. Chem. Lett*, vol. 13, p. 657, 2003.

[24] D. Shashank, T. Vishawanth, M. Arif Pasha et al., "Synthesis of some substituted benzothiazole derivaties and its biological activities," *International Journal of ChemTech Research*, vol. 1, no. 4, pp. 1224–1231, 2009.

[25] C. Papadopoulou, A. Geronikaki, and D. Hadjipavlou-Litina, "Synthesis and biological evaluation of new thiazolyl/benzothiazolyl-amides, derivatives of 4-phenyl-piperazine," *II Farmaco*, vol. 60, no. 11-12, pp. 969–973, 2005.

[26] E. Theophil and H. Siegfried, *The Chemistry of Heterocycles Structure: Reactions, Syntheses, and Applications*, Wiley-VCH, Verlag GmbH, and Co., Weinheim, Germany, 2nd edition, 2003.

[27] B. S. Dawane, S. G. Konda, V. T. Kamble, S. A. Chavan, R. B. Bhosale, and B. M. Shaikh, "Multicomponent one-pot synthesis of substituted hantzsch thiazole derivatives under solvent free conditions," *E-Journal of Chemistry*, vol. 6, no. 1, pp. S358–S362, 2009.

[28] D. Lednicer, L. A. Mitscher, and G. I. Georg, *Organic Chemistry of Drug Synthesis*, vol. 4, John Wiley & Sons, Inc., New York, NY, USA, 1990.

[29] K. S. Kim, S. D. Kimball, R. N. Misra, D. B. Rawlins et al., "Discovery of aminothiazole inhibitors of cyclin-dependent kinase 2: synthesis, X-ray crystallographic analysis, and biological activities," *J. Med. Chem*, vol. 45, no. 18, pp. 3905–3927, 2002.

[30] O. Annen, R. Egli, R. Hasler, B. Henzi, H. Jakob, and P. Matzinger, "Replacement of disperse anthraquinonedyeS," *Review of Progress in Coloration and Related Topics*, vol. 17, no. 1, pp. 72–85, 1987.

[31] L. Shuttleworth and M. A. Weaver, *The Chemistry and Application of Dyes*, Plenum Press, New York, NY, USA, 1990.

[32] M. J. Frisch, G. W. Trucks, H. B. Schlegel et al., Gaussian, Inc., Wallingford CT, 2016.

[33] P. Geerlings, F. de Proft, and W. Langenaeker, "Conceptual density functional theory," *Chemical Reviews*, vol. 103, no. 5, pp. 1793–1874, 2003.

[34] Foresman J. B. and A. Frisch, *Exploring chemistry with electronic structure methods*, Gaussian, Inc., Wallingford, CT, USA, 3rd edition, 2015.

[35] I. Fleming, *Frontier Orbitals and Organic Chemical Reactions*, John Wiley and Sons, New York, NY, USA, 1976.

[36] L. R. Domingo, E. Chamorro, and P. Pérez, "Understanding the reactivity of captodative ethylenes in polar cycloaddition reactions. A theoretical study," *Journal of Organic Chemistry*, vol. 73, no. 12, pp. 4615–4624, 2008.

[37] L. R. Domingo, M. Ríos-Gutiérrez, and P. Pérez, "Applications of the conceptual density functional theory indices to organic chemistry reactivity," *Molecules*, vol. 21, no. 6, article no. 748, 2016.

[38] L. R. Domingo, "A new C-C bond formation model based on the quantum chemical topology of electron density," *RSC Advances*, vol. 4, no. 61, pp. 32415–32428, 2014.

[39] L. R. Domingo, "Molecular electron density theory: a modern view of reactivity in organic chemistry," *Molecules*, vol. 21, no. 10, article no. 1319, 2016.

[40] F. Zielinski, V. Tognetti, and L. Joubert, "Condensed descriptors for reactivity: a methodological study," *Chemical Physics Letters*, vol. 527, pp. 67–72, 2012.

[41] JS. Murray and K. Sen, *Molecular Electrostatic Potentials, Concepts and Applications*, Elsevier, Amsterdam, Netherlands, 1996.

[42] P. Politzer and J. S. Murray, "The fundamental nature and role of the electrostatic potential in atoms and molecules," *Theoretical Chemistry Accounts*, vol. 108, no. 3, pp. 134–142, 2002.

[43] J. S. Murray and P. Politzer, "The electrostatic potential: an overview," *Wiley Interdisciplinary Reviews: Computational Molecular Science*, vol. 1, no. 2, pp. 153–163, 2011.